CHEMICAL ENGINEERING TRANSACTIONS
VOL. 103, 2023
A publication of AIDIC
The Italian Association of Chemical Engineering
Online at www.cetjournal.it
Guest Editors: Petar S. Varbanov, Panos Seferlis, Yee Van Fan, Athanasios Papadopoulos

ISBN 979-12-81206-02-1; **ISSN** 2283-9216
DOI: 10.3303/CET23103077

Fluid Flow and Heat Transfer CFD Analysis Inside Solar Flat Plate Collectors

Keivan Haghverdi[a], Georgios Martinopoulos[a], Dimitrios Misirlis[b,*]

[a]School of Science and Technology, UCIPS, International Hellenic University, Thessaloniki, Greece
[b]Department of Mechanical Engineering, International Hellenic University, 62124 Serres, Greece
dmissirlis@ihu.gr

The effectiveness and affordability of solar thermal collectors must increase to promote solar thermal energy systems further. To accomplish this, it is vital to make use of tools which enable the evaluation and potential optimization of the effectiveness of new designs. By concentrating on the computational (CFD) analysis of a direct absorption polymer (polycarbonate) flat plate solar collector's performance, this paper illustrates such an endeavor. The adoption of the suggested material may lead to the manufacture of flat plate collectors that are both more economical and environmentally friendly. The most important aspect in the performance of this collector focuses on the efficient solar energy absorption by the working fluid. This energy transfer is accomplished by employing a clear polymer honeycomb structure inside the collector. Inside the polymer honeycomb structure channels, solar energy is absorbed directly by the working fluid. For the maximization of energy efficiency, it is important to assess and optimize the flow field development and heat transfer inside the collector. For this reason, a CFD model of the solar collector was created in the commercial CFD software Ansys CFX. The model included all the basic geometrical and thermophysical characteristics defining the fluid flow and heat transfer taking place in the solar collector, also taking into consideration buoyancy and gravity effects. For the proper inclusion of the effect of the internal polymer honeycomb structure in the CFD model, a porous medium approach was adopted, and appropriate source terms were added in the Navier-stokes equations through which the macroscopic effect on the fluid flow development and heat transfer could be sufficiently captured. CFD computations were performed to investigate the temperature, velocity, and pressure patterns in different regions of the solar collector, and a broader insight regarding the flow field and heat transfer inside the solar collector design was achieved. The CFD results were also compared with reasonable agreement with available experimental and simulation data from the literature. The numerical results showed an acceptable performance of this polymer design in relation to more standard designs. The results also revealed some weak points of the design, such as the identification of recirculation regions which can be the target of future optimization actions in future works.

1. Introduction

Currently, renewable energy sources utilization is one of the key parameters for sustainable development (Gielen et al., 2019). Awareness regarding environmental issues such as pollution and global warming is of prime importance since renewable energy sources have a low carbon footprint, an attribute that makes them more environmentally friendly in comparison to fossil-based sources of energy (Hao et al., 2023). One of the most important renewable energy sources is solar energy, with the most used methods to exploit it being either photovoltaics that convert solar radiation to electricity or solar thermal collectors in order to absorb solar radiation and convert it to heat. This is usually accomplished with the aid of a heat transfer fluid flowing inside the solar thermal collector (Martinopoulos, 2018). The heated fluid can be either used directly or stored in a thermal storage tank, from which it can be used later (usually for time periods when solar energy potential is reduced). Researchers have utilized different approaches to optimize flat plate collectors, with CFD and finite element modeling being at the forefront in recent years. Do Ango et al. (2013) used numerical analysis of a novel solar collector design to determine the effects of various design parameters (air gap thickness, collector length) and operating factors (mass flow rate, incoming solar energy, inlet temperature) on the collector's instantaneous

Paper Received: 14 April 2023; Revised: 02 July 2023; Accepted: 24 July 2023
Please cite this article as: Haghverdi K., Martinopoulos G., Misirlis D., 2023, Fluid Flow and Heat Transfer CFD Analysis Inside Solar Flat Plate Collectors, Chemical Engineering Transactions, 103, 457-462 DOI:10.3303/CET23103077

efficiency. CFD simulation is used to examine the important effects of the inclination of the solar collector, the mass flow rate of the incoming heat removal fluid, and the distance of the air gap on the solar collector collection efficiency by other researchers (Wang et al., 2015). In another study (Gunjo et al., 2017), experimental values for solar radiation, ambient temperature, and heat transfer fluid temperature at the intake were utilized, along with ANSYS Fluent, to forecast the Nusselt number, heat transfer coefficient, and heat transfer fluid temperature at the exit of a solar collector. To minimize the economic and environmental cost of solar collectors (Martinopoulos et al., 2010), the use of polymers for the absorber is actively researched (Selinkov et al., 2022). The present work is focused on the CFD investigation of the thermal performance of a novel polymer flat plate solar collector (Martinopoulos et al., 2010). The main target of this work focuses on the process of direct absorption of solar radiation by the working fluid to assess the collector thermal performance and, a next step, investigate the possibility of using such solar flat plate collector designs as more cost-efficient and yet, environmentally friendlier, flat plate collectors.

2. The solar flat plate thermal collector geometry

The solar flat plate thermal collector that will be computationally investigated in the present work was originally proposed as a polymer solar collector with hopes of further reducing the production and maintenance costs while keeping the efficiency of the system on the same level as that found in the classic types of flat plate collectors. The overall solar flat plate collector geometry (Figure 1) is based on the experimental setup presented by Martinopoulos et al. (2010).

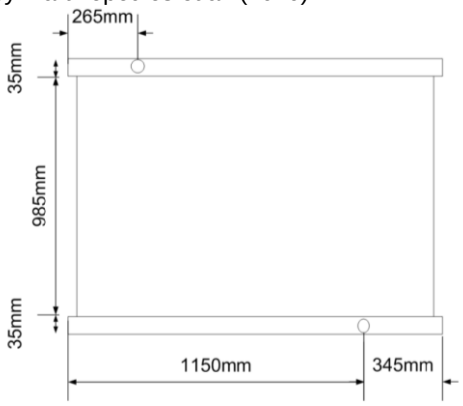

Figure 1: Overall solar flat plate collector geometry (Martinopoulos et al., 2010)

As can be seen, the flat plate collector's height is 1,055 mm, and its width is 1,495 mm. At the top and bottom of the collector, there are two horizontal headers, each comprising a rectangular 8 mm acrylic duct. The heat transfer fluid enters the collector through the inlet pipe, which is connected to the bottom header at a distance of 345 mm from the corner of the collector. From the bottom header, the heat transfer fluid is distributed throughout the collector channels. After the transfer fluid is heated by solar energy in the collector channels, its density is reduced and moves upward until it reaches the top header. The top header is connected to the outlet pipe, which is located at a distance of 265 mm far from the opposite top corner. Then, the heat transfer fluid exits the collector by the outlet pipe and moves to the storage tank. The main collector area is occupied by a polymer honeycomb structure composed of rectangular transparent channels, in which heat is directly transferred to the heat transfer medium. Figure 2 shows a typical view of the honeycomb collector geometry.

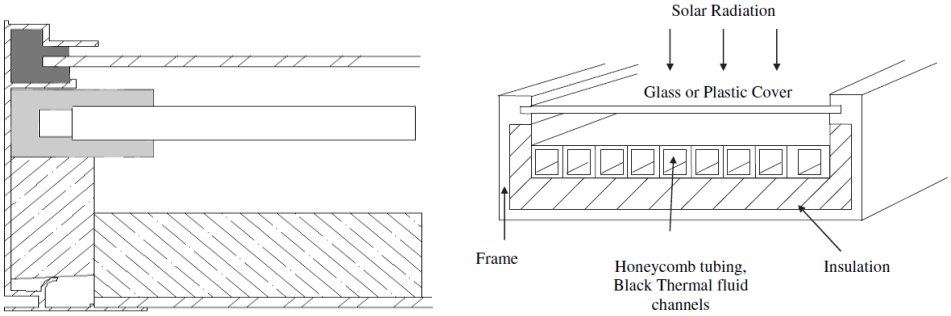

Figure 2: View of a cross-section of the flat plate solar collector (Martinopoulos et al., 2010)

3. The solar collector CFD model

The solar collector geometry of the CFD model is presented in Figure 3 and consists of 5 separate geometrical domains, i.e., the inlet pipe, the bottom header, the collector main area (the area with the honeycomb rectangular structures channels), the top header, and the outlet pipe. The top and bottom headers are rectangular and horizontally located on the top and bottom of the system. The headers have an 8 x 8 mm square face on the sides with a length of 1,495 mm. The inlet and outlet pipes are cylindrical pipes and are connected to the headers at specific positions. The radius of the inlet and outlet pipes is 3.5 mm, with a length of 50 mm. At the next step, a detailed CFD model of ~500,000 computational nodes was created in the Ansys Workbench CFD platform. Typical views of the CFD model are presented in Figure 3, where the computational domain overall geometry and the grid at the pipes and the collector main area are presented. As it can be seen, in the pipe regions, the grid is denser, with a higher number of computational nodes near the pipe wall to improve the boundary layer resolution. The same level of attention was applied near the front side of the collector, which represents the collector absorber plate and is modeled as a wall with constant heat flux. Regarding the collector main area, it should be mentioned that the CFD model does not contain the detailed geometry of the honeycomb rectangular channel since this would lead to a computationally unaffordable number of computational nodes. To compensate for this problem, the collector main area is being modeled as a porous medium having predefined pressure drop macroscopic performance.

The porous medium methodology is particularly useful for cases when the flow field geometry is too detailed or complicated to be precisely modeled (e.g., in cases where a high number of channels is presented) and would require an extremely high number of computational points, which would be computationally unaffordable. The effect of the (not-included in the CFD modeling) detailed geometry on the pressure drop is described by typical equations describing the pressure drop inside pipes. These equations are included as additional terms in the Navier-Stokes equations, which describe the flow field development. Based on the CFD solution with the adapted (including these source terms) Navier-Stokes equations, the flow field can be calculated in a way that the detailed geometry effect can be sufficiently captured, as also presented in the literature (Martinopoulos et al., 2010).

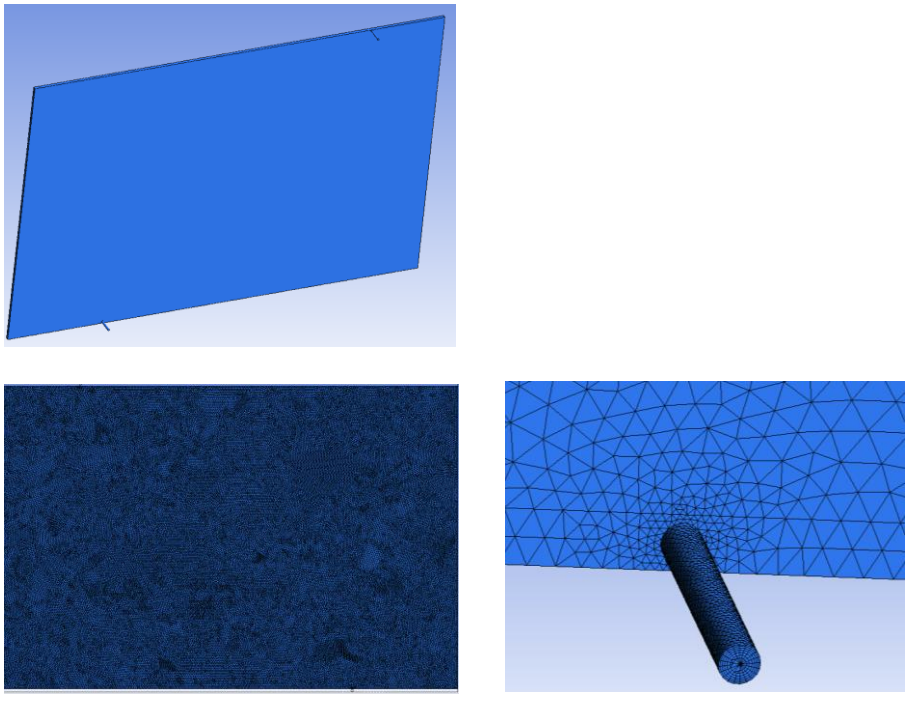

Figure 3: Typical views of the computational domain and the computational grid

The effect of the honeycomb rectangular structure on the flow field development is quantified by the addition of appropriate source terms, S_{total_x} , S_{total_y} and S_{total_z} , in the Navier-Stokes momentum equations as shown in Eq.(1), where u, v, and w correspond to the x,y and z velocity components. The general formulation of the total source terms in each flow direction is represented in Eq.(2) while Eq.(3) and Eq.(4) present the details of each source term. More specifically, the source term, S_{Y_PM} , is modelling the effect of the honeycomb structure

rectangular channels on the pressure drop (for laminar flow conditions), while for the source terms, S_{X_PM} and S_{Z_PM} extremely high values are being arbitrarily applied in order to make the flow become aligned to the y direction and model the fact that due to its structure the flow cannot move in the x and z directions inside the honeycomb structure channels. The effect of buoyancy and gravity is only considered in the y and z direction by the respective source terms $S_{y\_buoyancy}$ and $S_{z\_buoyancy}$, shown in Eq.(4) since the solar flat plate collector is inclined at a 60º angle as shown in Figure 4. Finally, in Eq.(5) ,the definition of the thermal expansion coefficient β is presented. It also needs to be mentioned that the source terms of Eqs.(1)–(5) are all fully applied in the collector main area domain (the area with the honeycomb rectangular channels) while in the inlet pipe, bottom header, top header and outlet pipe domains the source terms of Eq.(3) were not included since no honeycomb structure was present there and there was no need to model the additional pressure drop terms of Eq.(3). In these equations, μ corresponds to dynamic viscosity [Pa s], ρ to density [kg/m^3], p to pressure [Pa], T to temperature [K], D to diameter [mm], and Porosity refers to the honeycomb empty to total volume ratio. All values are in SI units. The source term units are in [N/m^3].

$$\begin{aligned}\frac{\partial(\rho u)}{\partial t}+\nabla.(\rho u\vec{u})&=-\frac{\partial p}{\partial x}+\nabla.(\mu\nabla u)+S_{total\_x}\\ \frac{\partial(\rho v)}{\partial t}+\nabla.(\rho v\vec{u})&=-\frac{\partial p}{\partial y}+\nabla.(\mu\nabla v)+S_{total\_y}\\ \frac{\partial(\rho w)}{\partial t}+\nabla.(\rho w\vec{u})&=-\frac{\partial p}{\partial z}+\nabla.(\mu\nabla w)+S_{total\_z}\end{aligned} \tag{1}$$

$$\begin{aligned}S_{total\_x}&=S_{x\_PM}\\ S_{total\_y}&=S_{y\_PM}+S_{y\_gravity}+S_{y\_buoyancy}\\ S_{total\_z}&=S_{z\_PM}+S_{z\_gravity}+S_{z\_buoyancy}\end{aligned} \tag{2}$$

$$\begin{aligned}S_{x\_PM}&=-10^{10}\mu u\\ S_{y\_PM}&=\frac{-32\mu v}{Porosity\times D^2}\\ S_{z\_PM}&=-10^{10}\mu w\end{aligned} \tag{3}$$

$$\begin{aligned}S_{y\_gravity}+S_{y\_buoyancy}&=-\rho g\sin\varphi\,(1-\beta(T-T_{ref}))\\ S_{z\_gravity}+S_{z\_buoyancy}&=-\rho g\cos\varphi\,(1-\beta(T-T_{ref}))\end{aligned} \tag{4}$$

$$\beta=-\frac{1}{\rho}\left(\frac{\partial\rho}{\partial T}\right)_P \tag{5}$$

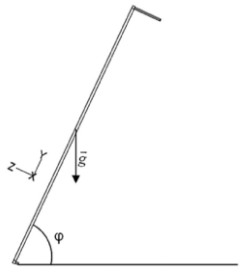

Figure 4: Solar flat plate collector inclination angle

For the modeling of the solar radiation effect to the solar collector model, a heat flux boundary condition was applied to the front face of the solar collector model, as presented in Eq.(6), which also includes the radiation heat loss from the sides of the collector. In Eq.(6) σ is the Stefan-Boltzmann constant, and ε is the emissivity of the wall, which was considered equal to 0.85. Additional details about the modeling procedure and the source terms formulation can be found in (Haghverdi, 2021).

$$TotalHeatflux[W/m^2]=Sun\,radiation[W/m^2]-\sigma(T_{wall}^4-T_{ref})\times\varepsilon \tag{6}$$

In the CFD computations a mixture of water with carbon ink was considered as the working fluid with temperature dependent properties shown below in Eqs.(7-9) for density ρ, dynamic viscosity μ and thermal conductivity k, respectively. The heat transfer medium heat capacity was considered as constant and equal to ~4,180 [J/(kgK)].

$$\rho(T) = 0.003284948 \times T^2 + 1.687644 \times T + 785.6677 \quad (7)$$

$$\mu(T) = 1.406 \times 10^{-7} \times T^2 - 0.0001024062 \times T + 0.01895682 \quad (8)$$

$$\mathrm{K(T)} = 9.8135 \times 10^{-6} \times T^2 + 0.007536807 \times T - 0.7674181 \quad (9)$$

4. CFD results

At the next step, CFD computations were performed in Ansys CFX software. Regarding the boundary conditions, at the inlet of the computational domain, the normal velocity to the inlet was set equal to 0.77 m/s, and the inlet temperature was set equal to 303 K. At the outlet of the computational domain, the static pressure was set equal to 10^5 Pa. Finally, regarding the heat flux, it was set equal to 900 W/m^2. All these values were selected to match the parameters used in the experimental study done by Martinopoulos et al. (2010). It also needs to be mentioned that for these conditions, the flow inside the honeycomb rectangular channels is positioned within the laminar regime. The CFD computations were performed with the use of 2nd order high-resolution advection schemes. The CFD computations converged smoothly after ~20,000 iterations for the momentum, mass, and energy equations. A typical view of the temperature distribution CFD results at the middle plane of the flat plate solar collector is presented in Figure 5 (top figure). As can be seen, the overall look of this temperature pattern is in very good agreement with the infrared photo taken from the experimental work presented in (Martinopoulos et al., 2010), presented in Figure 5 (bottom figure). Regarding the pressure distribution, presented in Figure 6, the CFD model also presents similar patterns as the ones in the work of Martinopoulos et al. (2010).

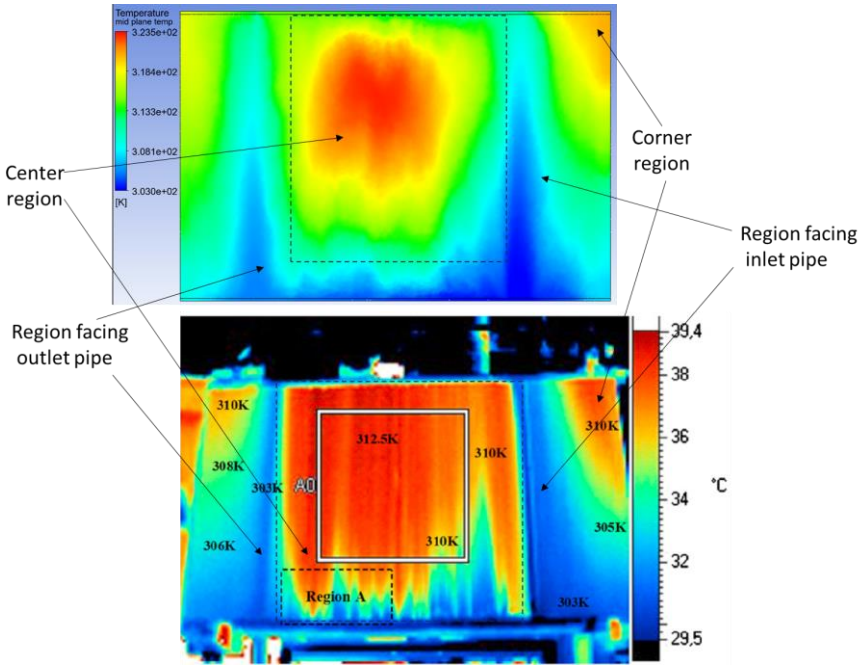

Figure 5: Solar flat plate collector temperature distribution, top: CFD computations (in the middle plane), bottom: Experimental model temperature distribution (Martinopoulos et al., 2010)

More specifically, as can be seen, a large area in the middle-top of the collector presents the highest temperature values. This region is limited by two lower-temperature regions, which are aligned with the positioning of the inlet and outlet pipes. In general, similar temperature patterns are shown in Figure 5. Similar temperature patterns can be identified in the Centre region, Corner region, and the Regions facing the inlet and outlet pipes (as indicated in Figure 5). The reason for the different temperature values is attributed to different levels of the inlet heat transfer medium temperature, which was higher at the CFD computations by ~ 10 K, which is approximately equal to the difference in the inlet temperature level, as also shown in Table 1.

Table 1: Comparison of temperature between CFD and Experiments (values in K)

	Inlet temperature	Center region	Corner region
CFD	303	323.5	320
Experiment	293	312.5	310

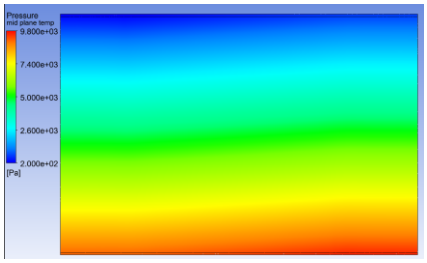

Figure 6: Solar flat plate collector pressure distribution in relation to 1atm (in the middle plane)

5. Conclusion

In the present work, a CFD model of the flat plate solar polymer collector was created in the CFD software Ansys CFX and validated by comparing it with experimental and simulation data available in the literature. The CFD model was based on the adoption of a porous medium approach through which all the important geometrical and thermophysical heat transfer and fluid flow characteristics of the detailed solar collector could be incorporated into the computational analysis in a computationally affordable manner. More specifically, the effect of the polymer honeycomb structure, based on rectangular channels, was included in the CFD model by the incorporation of appropriate, direction-dependent source terms, which were added in the Navier-stokes equations. Through these source terms, the macroscopic effect of fluid flow and heat transfer behavior of the collector geometry could be sufficiently captured while, at the same time, important temperature and pressure patterns could be properly computed in a computationally affordable manner. A first-step comparison of the CFD results in relation to experimental data was performed, indicating that the CFD model was, in general, capable of capturing the macroscopic flow and heat transfer characteristics of the flat plate solar collector. The CFD results provided similar temperature distribution in relation to the literature available experimental data, and the same problematic regions in the collector area were identified. The model can be used as a useful future optimization tool, similar to the approach presented in the work of (Martinopoulos et al. 2014), which was developed in Ansys Fluent software, to investigate the performance of various solar flat plate collector designs to conclude the most promising ones in terms of efficiency and solar energy capturing.

References

Do Ango A.M., Médale M., Abid C., 2013, Optimization of the design of a polymer flat plate solar collector. Solar Energy, 87, 64-75.

Gielen D., Boshell F., Saygin D., Bazilian M.D., Wagner N., Gorini R., 2019, The role of renewable energy in the global energy transformation. Energy Strategy Reviews, 24, 38-50.

Gunjo D.G., Mahanta P., Robi P.S., 2017, CFD and experimental investigation of flat plate solar water heating system under steady state condition. Renewable Energy, 106, 24-36.

Haghverdi K., 2021, CFD Investigation Inside Solar Flat Plate Collectors, MSc Dissertation, International Hellenic University, Thessaloniki, Greece.

Hao Y., Li X., Murshed M., 2023, Role of environmental regulation and renewable energy technology innovation in carbon neutrality: A sustainable investigation from China. Energy Strategy Reviews, 48, 101114.

Martinopoulos G., Missirlis D., Tsilingiridis G., Yakinthos K., Kyriakis N., 2010, CFD Modeling of a Polymer Solar Collector. Renewable Energy, 35, 1499–1508.

Martinopoulos G., 2018, Life Cycle Assessment of solar energy conversion systems in energetic retrofitted buildings. Journal of Building Engineering, 20, 256-263.

Wang N., Zeng S., Zhou M., Wang S., 2015, Numerical study of flat plate solar collector with novel heat collecting components. International Communications in Heat and Mass Transfer, 69, 18-22.